Superconducting nanowire single photon detector on diamond

Haig A. Atikian, Amin Eftekharian, A. Jafari Salim, Michael J. Burek, Jennifer T. Choy, A. Hamed Majedi, and Marko Lončar

Articles you may be interested in

Inhomogeneous critical current in nanowire superconducting single-photon detectors
Appl. Phys. Lett. **105**, 222602 (2014); 10.1063/1.4903071

Superconducting nanowire single photon detectors fabricated from an amorphous Mo0.75Ge0.25 thin film
Appl. Phys. Lett. **105**, 022602 (2014); 10.1063/1.4890277

Characterization of superconducting nanowire single-photon detector with artificial constrictions
AIP Advances **4**, 067114 (2014); 10.1063/1.4881981

Investigations of afterpulsing and detection efficiency recovery in superconducting nanowire single-photon detectors
J. Appl. Phys. **113**, 213102 (2013); 10.1063/1.4807833

Optimisation of NbN thin films on GaAs substrates for in-situ single photon detection in structured photonic devices
J. Appl. Phys. **113**, 143507 (2013); 10.1063/1.4800838

Superconducting nanowire single photon detector on diamond

Haig A. Atikian,[1] Amin Eftekharian,[2,3] A. Jafari Salim,[2,3] Michael J. Burek,[1]
Jennifer T. Choy,[1] A. Hamed Majedi,[2,3] and Marko Lončar[1,a)]

[1]*School of Engineering and Applied Sciences, Harvard University, 33 Oxford Street, Cambridge, Massachusetts 02138, USA*
[2]*University of Waterloo, 200 University Ave West, Waterloo, Ontario N2L 3G1, Canada*
[3]*Institute for Quantum Computing, University of Waterloo, 200 University Ave West, Waterloo, Ontario N2L 3G1, Canada*

Superconducting nanowire single photon detectors are fabricated directly on diamond substrates and their optical and electrical properties are characterized. Dark count performance and photon count rates are measured at varying temperatures for 1310 nm and 632 nm photons. A multi-step diamond surface polishing procedure is reported, involving iterative reactive ion etching and mechanical polishing to create a suitable diamond surface for the deposition and patterning of thin film superconducting layers. Using this approach, diamond substrates with less than 300 pm Root Mean Square surface roughness are obtained. © 2014 AIP Publishing LLC.
[http://dx.doi.org/10.1063/1.4869574]

Diamond has recently gained significant interest as a promising platform for on-chip high-performance photonic devices.[1–3] Diamond exhibits many favorable material properties such as a high refractive index (n = 2.4), wide bandgap (5.5 eV), and a large optical transmission range from the UV to the mid infrared. Diamond is also host to numerous defect color centers such as the nitrogen-vacancy (NV) center that can be utilized as an optically addressable spin based memory, particularly interesting in the field of quantum information processing.[4,5] In addition, diamond has a relatively large Kerr non-linearity[6] ($n_2 = 1.3 \cdot 10^{-19}$ m^2/W) making it an attractive platform for on-chip nonlinear optics in the visible and infrared wavelengths.[7] An exciting application for utilizing this diamond non-linearity could allow for frequency conversion of photons generated by color centers in diamond, which typically emit in the visible range, to the telecom wavelengths.[8] This could enable transmission of quantum information and distribution of quantum entanglement[9,10] over long distances, for the realization of quantum repeaters. Such an integrated diamond quantum photonics platform would benefit from the realization of high performance single photon detectors, with broadband photon sensitivity, that are integrated directly on the same diamond chip.

Superconducting nanowire single photon detectors (SNSPDs) outperform other single photon detector technologies on several merits such as quantum efficiency,[11] timing jitter, dark count rates, and broad spectral sensitivity.[12,13] SNSPDs typically consist of narrow width nanowires patterned into an ultrathin (4 nm to 8 nm) superconducting film, commonly made from niobium nitride or some derivative of.[14] The nanowires are current biased close to the critical current of the superconductor. When an incident photon is absorbed by the wire, a small resistive hotspot is formed generating a voltage pulse that can be subsequently amplified and measured.[15] Since the performance of SNSPDs is critically dependent on nanowire structural uniformity, it is

crucial to have them deposited on smooth substrate surfaces to avoid constrictions that can have detrimental effects on detection efficiency.[16]

In this letter, we report NbTiN superconducting nanowires deposited directly on diamond substrates that exhibit promising single photon sensitivity. Specifically, we provide details of the fabrication procedure developed, resulting in smooth diamond surfaces suitable for deposition of high-quality superconducting thin films. Furthermore, we show experimental data on the temperature performance of the SNSPDs on diamond substrates irradiated by 632 nm and 1310 nm photons. The performance of the devices is comparable to the performance of SNSPDs fabricated on conventional substrates such as sapphire, MgO, and silicon.[12]

We use type IIa single crystal diamond substrates cut in the {100} crystallographic orientation, obtained from Element Six, which were grown using microwave assisted CVD. The "as received" diamond is polished along random crystal directions leading to the rough surface seen in Fig. 1(a). Diamond polishing involves sliding the diamond specimen on a cast iron wheel called a "scaife" charged with diamond powder at high pressures and high velocities. A terminology used in the polishing industry and scientific literature refers to the direction of the highest polishing wear rate (in the case of our IIa diamond samples the ⟨100⟩ direction on the {100} crystal plane), as the "easy direction" and the direction with the lowest polishing wear rate (in our samples the ⟨110⟩ or ⟨111⟩ direction in the {100} crystal plane) the "hard direction". Work by Grillo and Field[17] showed that when polishing {100} diamonds in the ⟨110⟩ direction, or the "hard direction," the polishing debris consists of fragments of diamonds, suggesting the material is being removed by mechanically chipping the surface. This is clearly seen in Fig. 1(a) where large chips, several microns in size, are seen on the diamond surface. They also showed that when polishing {100} diamond in the ⟨100⟩ direction, or the "easy direction," the wear debris mostly consisted of less dense forms of sp^2 carbon material, where material can be removed

a)loncar@seas.harvard.edu

more efficiently without chipping. The randomly oriented striations seen on the diamond surface also suggests how the polishing was done without aligning the diamond to its "easy direction" and leading to the hatch patterned polishing lines seen in Fig. 1(a).

Since the surface of these diamonds are typically damaged and highly strained due to the mechanical nature of cutting and polishing, the surface must be prepared before deposition of the superconducting thin film. The first step is an acid clean to remove the surface contaminants from the diamond. The diamonds are cleaned in a 1:1:1 refluxing mixture of sulfuric, nitric, and perchloric acid for approximately 1 h. Fig. 1(a) shows an atomic force microscopy (AFM) image of the diamond surface, as received from Element Six, after the acid clean. It exhibits a root mean square (RMS) surface roughness of $\sim$30 nm, with some clear chipped surface defects. This AFM image is corroborated by previous works done on diamond polishing.[18] This surface is clearly not suitable to deposit thin film superconductors, further steps are required to prepare an appropriate diamond surface.

The next step is to remove several microns from the surface layer of the diamond to be clear of any mechanically strained areas caused by the polishing process. This is achieved by using a two step reactive ion etching (RIE) pre-etch process. We first use a 30 min Ar/Cl_2 etch, followed by another 30 min of O_2 etch in the UNAXIS Shuttleline inductively coupled plasma (ICP) RIE. The resulting diamond surface can be seen in Fig. 1(b). Many rounded deep etch pits are formed in the diamond on the order of 100s of nanometers. These etch pits are believed to be formed in the vicinity of the defects on the original diamond surface created by polishing. The damaged areas etch at a different rate than the more dense diamond regions creating this cratered surface profile.

Following the RIE step, the diamond is re-polished along its "easy direction" to prepare a smooth surface. This second mechanical polishing step reduces the RMS surface roughness to the order of 1–2 nm as seen in Fig. 1(c). The polishing striations seen in this figure are all aligned in the same direction, which is a strong indication that the polishing was carefully performed along the "easy direction". Since the thickness of our superconducting nanowires is typically around 5 nm, having a surface roughness in this range would still be detrimental to device performance. Therefore, we follow this step with another acid clean with the same conditions as before to remove surface contaminants from the polishing process, and perform another RIE etch again with 30 min of Ar/Cl_2 and 30 min of O_2. This RIE etch is used to access a portion of the diamond that is clear of mechanical stress created by polishing, and to further average out the surface roughness via the ICP.[19] The final surface is seen in Fig. 1(d) where the RMS surface roughness is $\sim$150–300 pm, depending on the sample, for an area without any of the small circular defects. A large scan of the diamond chip showed that these small circular pit defects are sparsely present throughout the sample and typically 5 nm in depth. The probability of patterning a nanowire that does not intersect with one of these defects is quite high, and necessary to make a good device. Similar surface roughness was achieved in Ib diamonds using the procedure outlined above.

A NbTiN layer is deposited directly on the diamond surface by reactive sputtering using a Nb-Ti alloy target and a dc magnetron source. The Ar/N_2 partial pressure ratio and total pressure have been optimized to maximize critical temperature, and the substrates are held at ambient temperature. The critical temperature was measured to be 8.5 K, taken at the midpoint of the superconducting transition. Hydrogen silsesquioxane (HSQ) resist is used to pattern the nanowire
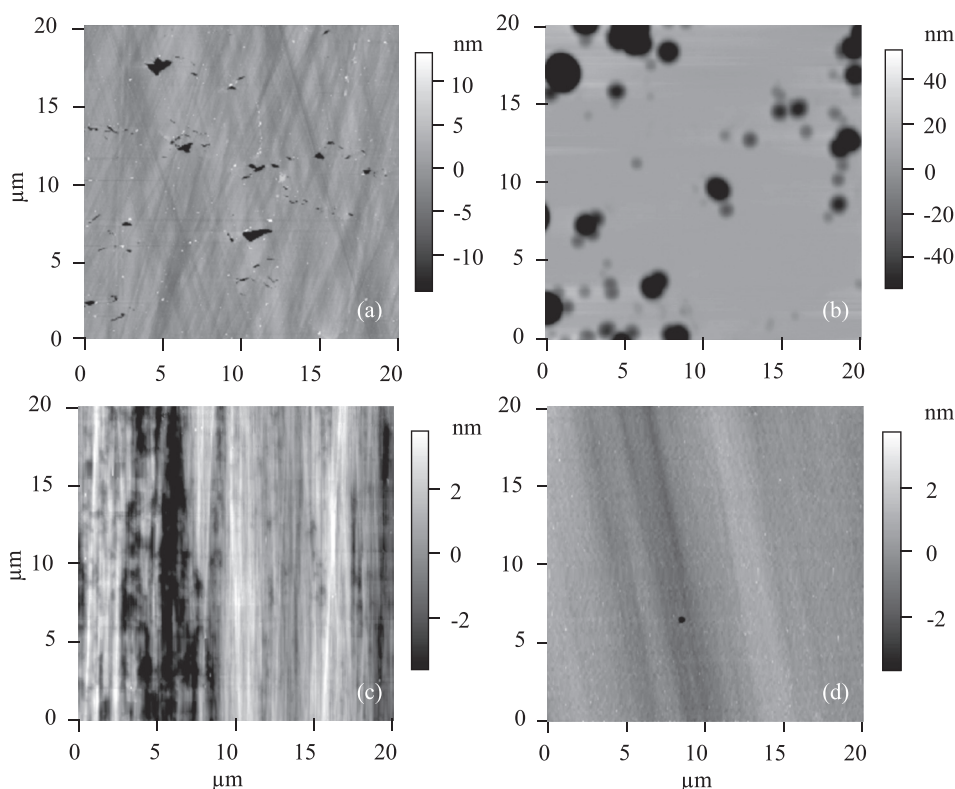

FIG. 1. (a) AFM image of a type IIa diamond surface from Element Six after acid cleaning in a 1:1:1 refluxing mixture of sulfuric, nitric, and perchloric acid with an initial RMS surface roughness of $\sim$30 nm. (b) AFM image of a IIa diamond surface after Ar/Cl_2 and O_2 RIE pre-etch. (c) AFM image of a IIa diamond surface after mechanical polishing with RMS surface roughness of 1–2 nm. (d) AFM image of the final type IIa diamond surface obtained after another Ar/Cl_2 and O_2 RIE with an RMS surface roughness of $\sim$ 300 pm.

structures using 125 keV electron-beam lithography. The resist is developed in a 25% tetra-methyl ammonium hydroxide solution, and the nanowire pattern is transferred into the film using ion beam milling with Argon gas.

A straight nanowire 10 μm long and 100 nm wide is connected to larger gold contact pads with a gradual taper to avoid any current crowding effects caused by bends and abrupt width variations.[20] The measurements were performed in a dipstick probe immersed in a Dewar of liquid helium. Each nanowire is connected to two series 470nH inductors (placed next to the sample) and to a room temperature bias-T via 50Ω coax cables. The inductors are utilized such that the electrical time constant is larger than the thermal time constant of the detector to avoid latching, ensuring the peak measured device current is the "experimental" critical current.[21] A computer controlled source meter (Keithley 2400) is connected to the DC port of the bias-T via a low pass filter. The high frequency pulses generated at the nanowire are amplified at room temperature and monitored on a high speed oscilloscope and programmable counter. A single mode fiber is placed several centimeters away from the sample, uniformly irradiating the sample with photons from an attenuated laser source.

Figure 2 illustrates the photon counting performance of a 100 nm wide, 6 nm thick nanowire on a diamond substrate irradiated by 1310 nm photons at varying temperatures. The impact of hotspot formation on the current distribution of the nanowire depends on the relative size of the generated hotspot area to the transverse dimension of the nanowire. In experiment, to have a device sensitive to single photons, the bias current is set close to the depairing current of the superconducting material. When the formation of the initial hotspot reaches its maximum effective size,[22,23] the local perturbation of current density is significant enough that a hotspot-driven photon-count event is triggered. For a bias current equal to or greater than this minimum value, all the photon absorptions are registered as photon-counts and hence the detector operates independent of the bias current. This behavior refers to the saturated area of quantum efficiency versus bias current observed in Figs. 2 and 3. In SNSPDs, even when the input optical terminal is fully blocked, randomly distributed signals are generated at the output electrical terminal of the detector for a particular current bias condition. Regardless of the nature of these thermal

FIG. 3. Count rate versus bias current at 4.2K for a 100 nm wide 6 nm thick nanowire irradiated by 632 nm photons. The straight line to the right represents the dark counts with no laser irradiation, while the left curve represents the count rate to an attenuated 632 nm laser source.

fluctuations, the rate always obeys the Kramers formula[24–26] which predicts an exponential dependence of the rate to the height of the potential barrier faced by these thermal fluctuations. Since this potential barrier is current dependent, a power law dependence is predicted for the dark count versus bias current measurement as observed in Fig. 2. These curves are indicative of a nanowire with uniform superconductive properties and no appreciable constrictions which have a drastic effect on photon counting performance.[16]

Fig. 3 illustrates the photon counting performance of a 100 nm wide, 6 nm thick nanowire on a diamond substrate irradiated by 632 nm photons at 4.2 K. The motivation is to show the nanowire's ability to detect photons emitted by NV centers in diamond with a zero-phonon line at 637 nm and phonon sideband from 640 to 780 nm. In this case of higher energy photons, the photo-generated hotspot has a greater effective size and can create a photon detection event at lower bias currents. Consequently, the count rate to 632 nm photons reaches a saturation level well before it intersects the dark count line even at 4.2 K. For NV applications these detectors can be biased at an operating point far from the critical current. Looking at Fig. 3, there exists a wide window where the detector can operate with practically zero dark counts, and a photon count rate in the saturated region with little influence to changes in bias current.

In conclusion, we have presented a method to prepare diamond surfaces with sub 300 pm RMS surface roughness suitable to deposit long superconducting nanowires for the purpose of single photon detection. We have also shown that the added challenges diamond presents to prepare its surface to a fine roughness does not hinder the performance of contemporary SNSPDs, and allow for easy integration of SNSPDs on nanoscale photonic devices carved out of single crystal diamond as the ones seen in Ref. 27. This approach is suitable for realization of a fully integrated quantum photonics platform based on diamond that leverages diamond's color centers as sources, and SNSPDs as detectors of single photons.
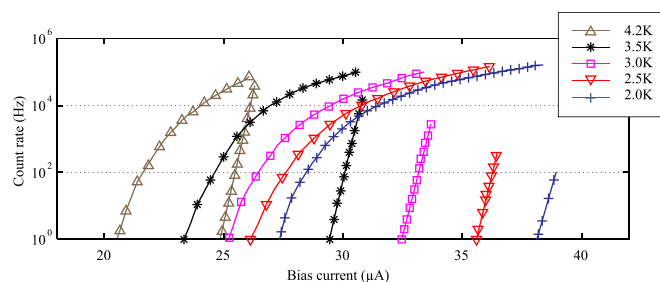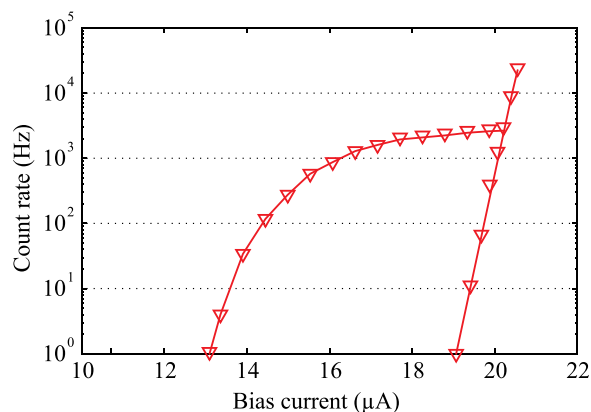
FIG. 2. Count rate versus bias current for a 100 nm wide 6 nm thick nanowire, for temperatures from 2 K to 4.2K. Each temperature data set has two curves represented by the same color and symbol. For each temperature, the straight line to the right represents the dark counts with no laser irradiation, while the left curve represents the count rate to an attenuated 1310 nm laser source.

[1]I. Aharonovich, A. D. Greentree, and S. Prawer, Nat. Photonics **5**, 397 (2011).

[2]B. Hausmann, J. Choy, T. Babinec, M. L. B. J. Shields, I. Bulu, and M. L. M. Lončar, Phys. Status Solidi A **209**, 1619–1630 (2012).

[3]M. Lončar and A. Faraon, MRS Bulletin **38**, 144 (2013).

[4]P. Neumann, N. Mizuochi, F. Rempp, P. Hemmer, H. Watanabe, S. Yamasaki, V. Jacques, T. Gaebel, F. Jelezko, and J. Wrachtrup, Science **320**, 1326 (2008).

[5]J. L. O'Brien, Science **318**, 1567 (2007).

[6]R. Boyd, *Nonlinear Optics* (Academic Press, 2008).

[7]B. Hausmann, I. Bulu, V. Venkataraman, P. Deotare, and M. Lončar, e-print arXiv:1309.1178.

[8]M. Raymer and K. Srinivasan, Phys. Today **65**(11), 32 (2012).

[9]E. Togan, Y. Chu, A. S. Trifonov, L. Jiang, J. Maze, L. Childress, M. V. G. Dutt, A. S. Sørensen, P. R. Hemmer, A. S. Zibrov *et al.*, Nature **466**, 730–734 (2010).

[10]H. Bernien, B. Hensen, W. Pfaff, G. Koolstra, M. S. Blok, L. Robledo, T. H. Taminiau, M. Markham, D. J. Twitchen, L. Childress *et al.*, Nature **497**, 86 (2013).

[11]F. Marsili, V. B. Verma, J. A. Stern, S. Harrington, A. E. Lita, T. Gerrits, I. Vayshenker, B. Baek, M. D. Shaw, R. P. Mirin *et al.*, Nat. Photonics **7**, 210 (2013).

[12]R. Hadfield, Nat. Photonics **3**, 696 (2009).

[13]M. Akhlaghi, H. Atikian, A. Eftekharian, M. Lončar, and A. Majedi, Opt. Express **20**, 23610 (2012).

[14]S. Dorenbos, E. Reiger, U. Perinetti, V. Zwiller, T. Zijlstra, and T. Klapwijk, Appl. Phys. Lett. **93**, 131101 (2008).

[15]G. Gol'tsman, O. Okunev, G. Chulkova, A. Lipatov, A. Semenov, K. Smirnov, B. Voronov, A. Dzardanov, C. Williams, and R. Sobolewski, Appl. Phys. Lett. **79**, 705 (2001).

[16]A. J. Kerman, E. A. Dauler, J. K. W. Yang, K. M. Rosfjord, V. Anant, K. K. Berggren, G. N. Gol'tsman, and B. M. Voronov, Appl. Phys. Lett. **90**, 101110 (2007).

[17]S. Grillo and J. Field, J. Phys. D: Appl. Phys. **30**, 202 (1997).

[18]S. Grillo, J. Field, and F. van Bouwelen, J. Phys. D: Appl. Phys. **33**, 985 (2000).

[19]C. L. Lee, E. Gu, M. D. Dawson, I. Friel, and G. A. Scarsbrook, Diamond Relat. Mater. **17**, 1292 (2008).

[20]J. Clem and K. Berggren, Phys. Rev. B **84**, 174510 (2011).

[21]A. Kerman, J. Yang, R. Molnar, E. Dauler, and K. Berggren, Phys. Rev. B **79**, 100509 (2009).

[22]A. N. Zotova and D. Y. Vodolazov, Phys. Rev. B **85**, 024509 (2012).

[23]A. Eftekharian, H. A. Atikian, and A. H. Majedi, Opt. Express **21**, 3043 (2013).

[24]L. N. Bulaevskii, M. J. Graf, and C. D. Batista, Phys. Rev. B **83**, 144526 (2011).

[25]H. Bartolf, A. Engel, A. Schilling, K. Il'in, M. Siegel, H.-W. Hübers, and A. Semenov, Phys. Rev. B **81**, 024502 (2010).

[26]T. Yamashita, S. Miki, K. Makise, W. Qiu, H. Terai, M. Fujiwara, M. Sasaki, and Z. Wang, Appl. Phys. Lett. **99**, 161105 (2011).

[27]M. Burek, N. de Leon, B. Shields, B. Hausmann, Y. Chu, Q. Quan, A. Zibrov, H. Park, M. Lukin, and M. Lončar, Nano Lett. **12**, 6084 (2012).